

Interaction of half-sandwich alkylmolybdenum(III) complexes with $B(C_6F_5)_3$. The X-ray structure of $[CpMo(\eta^4-C_4H_6)(\mu-Cl)(\mu-CH_2)(O)MoCp][CH_3B(C_6F_5)_3]$

Erwan Le Grogne^a, Rinaldo Poli^{a,*}, Philippe Richard^a, Rosa Llusar^b,
Santiago Uriel^b

^a Laboratoire de Synthèse et d'Electrosynthèse Organométalliques, Faculté des Sciences 'Gabriel', Université de Bourgogne, 6 Boulevard Gabriel, 21000 Dijon, France

^b Departament de Ciències Experimentals, Campus Riu Sec de la Universitat Jaume I, PO Box 224, 12080 Castelló, Spain

Received 31 May 2001; accepted 30 August 2001

Abstract

The reactions of the half-sandwich molybdenum(III) complexes $CpMo(\eta^4-C_4H_4R_2)(CH_3)_2$, where $Cp=\eta^5-C_5H_5$ and $R=H$ or CH_3 , with equimolar amounts of $B(C_6F_5)_3$ have been investigated in toluene. EPR monitoring shows the formation of an addition product which does not readily react with Lewis bases such as ethylene, pyridine, or PMe_3 . The analysis of the EPR properties and the X-ray structure of a decomposition product obtained from dichloromethane, $[CpMo(\eta^4-C_4H_6)(\mu-Cl)(\mu-CH_2)(O)MoCp][CH_3B(C_6F_5)_3]$, indicate that the borane attack has occurred at the methyl position. © 2001 Elsevier Science B.V. All rights reserved.

Keywords: Half-sandwich; X-ray structure; EPR properties; Molybdenum; Butadiene ligand

1. Introduction

Polymerization of α -olefins is one of the most important industrial processes. The combination of Group 4 metallocenes and methylaluminoxane (MAO) has been actively investigated in view of its homogeneous process and the possibility to control the stereoregularity of the polymerization though the control of the ligand architecture [1–5]. A few studies have also been carried out with isoelectronic Group 5 metal complexes such as $CpNb(\eta^4\text{-diene})R_2$ [6,7] and $Tp'Nb(\eta^2\text{-alkyne})R_2$ (Tp' = substituted hydrotris(pyrazolyl)borate) [8]. The prevalent concept of these works is the analogy (structure and electron count) to the architecture of the Group 4 metallocenes, where the 14 electron metallocene alkyl cation $[Cp_2MR]^+$ is the proposed active species [1,3,4]. By analogy with the work done on the Group 5 metals, we considered the possibility that the

half-sandwich 17-electrons molybdenum(III) complexes available in our laboratory [9,10] could also catalyze ethylene polymerization. Our initial experimental and theoretical studies of these complexes in ethylene polymerization catalysis have been recently reported [11]. In combination with methylaluminoxane, very low activities have been observed to yield polymers of high linearity and very high molecular weights. The theoretical studies have identified the low polarity of the $Mo-CH_3$ bonds, as compared with that of the $Nb-CH_3$ bonds in the analogous $Nb(III)$ derivatives, as the cause of the low activity because the activation process is made less favorable. Other strong organo-Lewis acids such as $B(C_6F_5)_3$ have also been used to generate the active species in situ [12]. Under the assumption that the active specie is the $[CpMo(\eta^4\text{-diene})R]^+$ complex, we were interested in probing the reactivity of the dimethyl complexes $CpMo(\eta^4\text{-diene})Me_2$ and Cp^* analogues with the methyl abstracting agent $B(C_6F_5)_3$ in order to evaluate the possibility to isolate the putative active species. The results of these investigations are reported in this contribution.

* Corresponding author. Tel.: +33-3-80396881; fax: +33-3-80396098.

E-mail address: rinaldo.poli@u-bourgogne.fr (R. Poli).

2. Results and discussion

The addition of one equivalent of $B(C_6F_5)_3$ to solutions of $CpMo(\eta^4\text{-diene})Me_2$ (diene = 1,3-butadiene or 2,3-dimethyl-1,3-butadiene) in toluene at $-20^\circ C$ leads to a rapid color change from green to orange. Analogous color changes were also observed upon treating the same Mo complexes with MAO [11]. In each case, the product appears stable at room temperature in hydrocarbon solvents and under an inert atmosphere, at least for a few days. Unfortunately, all our crystallization attempts (see Section 4) have yielded oily products. Therefore, the only information available to us on the nature of the reaction products comes from solution spectroscopic studies. Monitoring the reactions by EPR at $-20^\circ C$ shows that, in each case, the characteristic pseudo-binomial 11-line pattern of the dimethyl Mo(III) complex [10], due to the apparent equivalence of ten hydrogen atoms of the molecule, disappears and is replaced by a new, broader signal at $g = 1.995$. Both starting and final EPR spectra are essentially independent on the nature of the diene ligand, since the nature of the substitution of the diene ligand does not influence the g value nor the multiplicity of the spectrum. Fig. 1 shows the example of the butadiene system. The new signal is slightly broader than that of the starting complex and is characterized by a different coupling pattern.

Several adducts of $B(C_6F_5)_3$ with transition metal complexes have been characterized spectroscopically and, in a few cases, also by X-ray crystallography

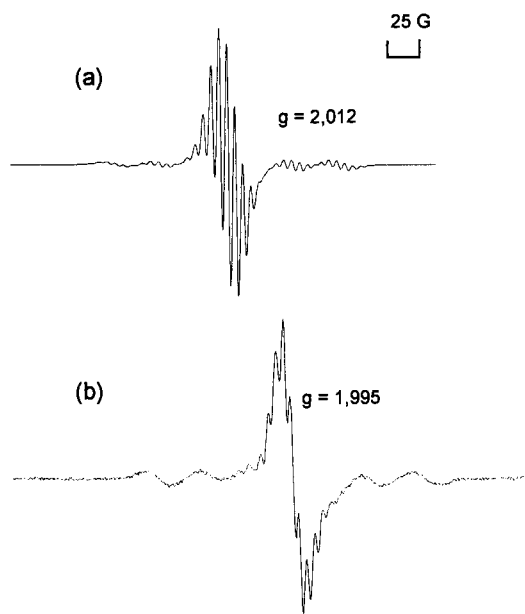


Fig. 1. EPR monitoring of the reaction between $CpMo(\eta^4\text{-C}_4\text{H}_6)Me_2$ and $B(C_6F_5)_3$ in toluene at $-20^\circ C$. (a) Before the borane addition. (b) After the borane addition.

[13–15]. The borane reagent unfailingly attacks an alkyl group whenever at least one is present, to generate a $M\cdots R\cdots B(C_6F_5)_3$ moiety where the $M-R$ bonding interaction is greatly weakened. In the presence of Lewis bases L (i.e. THF, pyridine, phosphines), sometimes even very weak ones such as organic halides, the alkyl is typically abstracted resulting in charge separation, to generate $[M(L)]^+[R-B(C_6F_5)_3]^-$ species [15–18]. However, boranes have also been shown to give rise to electrophilic additions to the terminal carbon atom of a coordinated diene to yield complexes containing a betaine allylic ligand, e.g. $M[\eta^3\text{-C}_3\text{H}_4\text{-CH}_2\text{B(C}_6\text{F}_5)_3]$ starting from a $M(\eta^4\text{-C}_4\text{H}_6)$ complex [19–24]. Therefore, the question of the site of attack (methyl or diene ligand) for complexes $CpMo(\eta^4\text{-C}_4\text{H}_6)Me_2$ is not a trivial one a priori. A good spectroscopic handle on the nature of the interaction is provided by ^{11}B - and ^{19}F -NMR, but this is unfortunately prevented in our case by the paramagnetism. The inability to observe a ^{19}F -NMR signal suggests, in fact, that the borane molecule is covalently linked to the paramagnetic Mo(III) complex.

The digital fitting of the EPR experimental spectrum provides useful information on the site of attack. The fitting was carried out only for the butadiene system, for which a slightly improved spectral resolution allowed a more accurate analysis. The fitting gives the best agreement for an $A_3M_3R_2X_2$ spin system (see Section 4). This is interpreted as resulting from two sets of three equivalent H atoms from the two chemically inequivalent methyl groups, plus two sets of two pseudo-equivalent H atoms from the two chemically distinct diene terminal (*syn* and *anti*) positions. Previous EPR studies of paramagnetic diene complexes have systematically shown coupling to the terminal *syn* and *anti* H atoms and no observable coupling to the internal H atoms [9,10,25–27]. Thus, the observed spectral modifications suggest that an interaction has occurred between the Lewis acid $B(C_6F_5)_3$ and one methyl group. The nonequivalence of the two methyl groups would then arise from the fact that one is bonded only to the Mo atom whereas the other one is bonded to the Mo and B atoms. This asymmetry should make the two opposite termini of the diene ligand also nonequivalent, giving rise to a $RSXY$ system rather than a R_2X_2 system for the diene H atoms. However, these atoms are far removed from the source of the asymmetry, yielding pseudo-equivalence, at least within the resolution limits of our spectrometer. Indeed, the quality of the fit significantly increases upon breaking the symmetry from 64 to 334 (the correlation increases from 0.990 to 0.992 and the error decreases from 1.743×10^{-2} to 1.342×10^{-2}). An almost insignificant improvement takes place upon further breaking the symmetry to 3322, because of the accidental equivalence of a_H to *syn* and *anti* diene protons. Previous studies have also

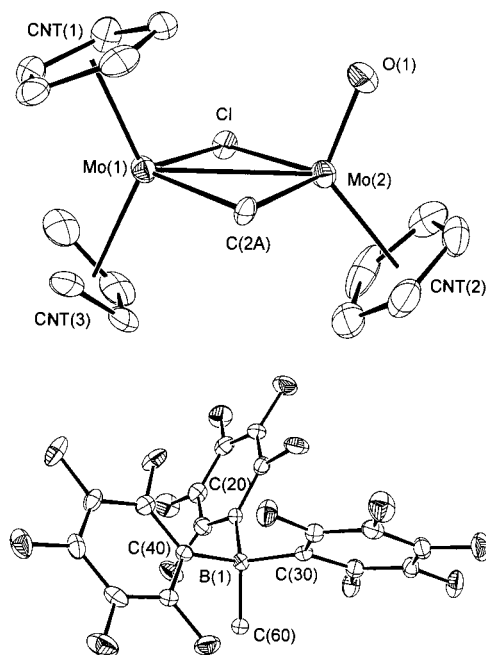


Fig. 2. An ORTEP view of cation (above) and anion (below) of compound $[\text{CpMo}(\eta^4\text{-C}_4\text{H}_6)(\mu\text{-Cl})(\mu\text{-CH}_2)(\text{O})\text{MoCp}][\text{B}(\text{C}_6\text{F}_5)\text{CH}_3]$ with thermal ellipsoids drawn at the 30% probability level.

highlighted the near-degeneracy of the hyperfine couplings to these two types of atoms [10,26,27]. Further lowering the symmetry to a 331111 spin system does not further improve the quality of the fit. The alternative interpretation of a borane attack at one of the diene termini seems less likely for two reasons. First, the diene terminal H spin system would be expected to show greater asymmetry. Second, and more importantly, the resulting betaine allyl ligand would show coupling to the *allylic* terminal H atoms (thus three rather than four H atoms), according to the available precedents for similar allylmolybdenum(III) complexes [27,28]. Attempts to simulate the EPR spectrum on the basis of a 33111 model, however, systematically gave unacceptable fits. It is to be noted that the a_{H} values for the two inequivalent methyl groups (6.79 and 4.42 G) are not too different from each other, suggesting that the borane-bonded methyl group is still solidly attached to the Mo center. This is consistent with the observed reactivity (or lack thereof), *vide infra*. For comparison, the a_{H} value for the methyl H atoms in dimethylmolybdenum(III) complexes are in the 5.3–6.3 G range, depending on the nature of the diene and cyclopentadienyl ligands [10,29]. The increased broadness of the spectrum relative to that of the starting dimethyl complex may be related to the onset of a dynamic exchange of the two methyl groups between the borane-bonded and nonbonded positions. A similar phenomenon has been shown to broaden the $^1\text{H-NMR}$ resonances for diamagnetic compounds having the

$\text{M}\cdots\text{R}\cdots\text{B}(\text{C}_6\text{F}_5)_3$ moiety [13,30,31]. The EPR spectrum recorded at different temperatures (both lower and higher) has a poorer resolution and no useful information could be obtained from its analysis.

Additional indication for the occurrence of a methyl rather than diene attack comes from previous computational investigations, showing that the Mulliken charge on the methyl ligands is more negative than that on the diene terminal position [11]. This is true also for the corresponding Nb system, for which the formation of the $[\text{CpNb}(\eta^4\text{-diene})\text{Me}]^+[\text{Me-MAO}]^-$ active site in ethylene polymerization catalysis has been proposed [7,32]. Finally, the borane attack at the methyl group for compound $\text{CpMo}(\eta^4\text{-C}_4\text{H}_6)\text{Me}_2$ is indicated by the characterization of the title compound, which results from a decomposition process (*vide infra*).

When the addition of $\text{CpMo}(\eta^4\text{-C}_4\text{H}_6)\text{Me}_2$ to the $\text{B}(\text{C}_6\text{F}_5)_3$ solution was followed by the addition of a slight excess of PMe_3 , no spectral modifications were observed by EPR. This surprising observation shows that the phosphine molecule is incapable of displacing the methyl group from either the boron atom [giving back the starting dimethyl Mo(III) complex and $\text{Me}_3\text{PB}(\text{C}_6\text{F}_5)_3$] or the molybdenum atom. The latter process would afford $[\text{CpMo}(\eta^4\text{-C}_4\text{H}_6)(\text{PMe}_3)\text{Me}][\text{MeB}(\text{C}_6\text{F}_5)_3]$ by substitution of the labile $[\text{CH}_3\text{B}(\text{C}_6\text{F}_5)_3]^-$ ligand with PMe_3 and should dramatically affect the shape of the EPR spectrum (notably a strong coupling to the P nucleus would be expected). A reaction of this type is undertaken, for instance, by the boratabenzene chromium complex $(\text{C}_5\text{H}_5\text{BMe})\text{Cr}(\text{Me})\{\text{MeB}(\text{C}_6\text{F}_5)_3\}$ upon addition of PMe_3 [18]. The resistance of the putative $\text{CpMo}(\eta^4\text{-C}_4\text{H}_6)\text{Me}\{\text{MeB}(\text{C}_6\text{F}_5)_3\}$ product against displacement of the borate anion is in agreement with the strength and low polarity of the Mo–CH₃ bonds in the half sandwich Mo(III) precursors, as indicated theoretically by DFT calculations [11] and experimentally by protonation studies [10].

Dissolution of the putative $\text{CpMo}(\eta^4\text{-C}_4\text{H}_6)\text{Me}\{\text{MeB}(\text{C}_6\text{F}_5)_3\}$ product in dichloromethane and diffusion of pentane, with participation of adventitious oxygen or water, afforded crystals of an oxygen and chlorine-containing decomposition product which were suitable for a full characterization, including an X-ray analysis. While the chlorine atom is obviously originating from the CH_2Cl_2 solvent, a likely source of the oxygen atom is residual water in the Celite used for the filtration. While oven-dried Celite was used and the product isolation was reproduced, omission of the filtration procedure only resulted in the formation of oily products. The compound corresponds to a salt of the dinuclear $[\text{CpMo}(\eta^4\text{-C}_4\text{H}_6)(\mu\text{-Cl})(\mu\text{-CH}_2)(\text{O})\text{MoCp}]^+$ cation and the $[\text{B}(\text{C}_6\text{F}_5)\text{CH}_3]^-$ anion. An ORTEP view of the two ions is shown in Fig. 2 and selected metric parameters are given in Table 1.

Cation and anion are well separated from each other in the unit cell. The minimum contact is 2.368 Å between atoms H4 and H60b. Very weak interactions are observed between two symmetry-related cations ($O1 \cdots H2$, 2.478 Å; $O1 \cdots H2-C2$, 146.1°), which are therefore pairwise arranged in the unit cell as shown in Fig. 3. The anion shows a regular tetrahedral coordination around the boron atom. The B–CH₃ distance of 1.658(6) Å is quite typical for this anion [33,34]. The cation is composed of the two fragments CpMo(η^4 -C₄H₆) and CpMo(O) bridged by a chlorine atom and a CH₂ group. The hydrogen atoms of the bridging methylene group were not directly located by the X-ray analysis, but their presence is unambiguously shown by the NMR characterization (vide infra). The central Mo₂(μ -Cl)(μ -CH₂) moiety is planar and the two Mo fragments are oriented in such a way as to place the two Cp rings on the opposite sides of the bridging plane (*anti*). The two metal atoms are sufficiently close to each other [2.8801(5) Å] to suggest the presence of a direct metal–metal interaction. The acute Mo–X–Mo angles at the bridging Cl and C(2A) atoms [72.00(4) and 86.62(3)°, respectively] reinforce this proposition.

Relative to the previously reported structure of CpMo(η^4 -C₄H₄Me₂-2,3)(CH₃)₂, the Mo(1)–CNT(1) distance (Mo–Cp centroid) is slightly shorter [1.985(4) vs.

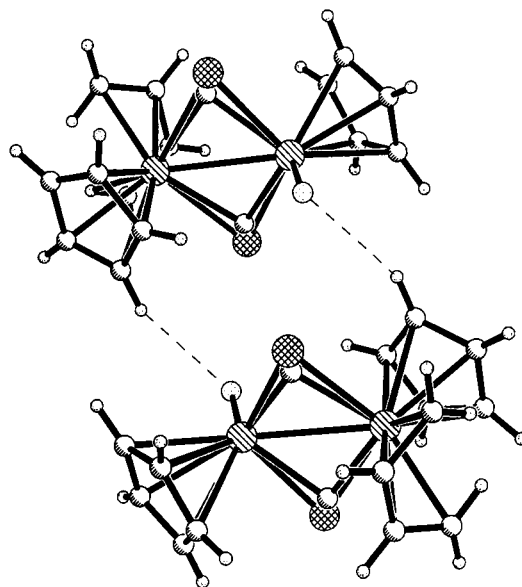


Fig. 3. A view of the pairwise arrangement of the dinuclear molybdenum cations.

2.019(5) Å], while the Mo(1)–CNT(3) distance (Mo–diene centroid) is slightly longer [1.964(4) vs. 1.925(3) Å], and the Mo(1)–C(2A) distance is considerably shorter relative to the two Mo–CH₃ distances [2.090(10) Å vs. an average of 2.225(3) Å]. A shortening of all distances to the (formally) anionic ligands and a lengthening of those to the neutral ones are expected when an oxidation state increase occurs. However, we should not assign, from this observation alone, a formal oxidation state IV to the Mo(1) center (and consequently an oxidation state IV also to the Mo(2) center). The alternative assignment as a III, V compound would also be consistent with the observed trends if we suppose that the presence of the adjacent Mo(V) center increases, via the bridging ligands and the direct metal–metal bond, the effective positive charge on the Mo(III) center. The Mo–X (bridging atom) distances to Mo(1) and Mo(2), however, are rather similar [2.497(2) vs. 2.401(3) Å for Cl, 2.090(10) vs. 2.108(15) Å for C(2A)], in better agreement with a IV, IV formulation. While the two Mo–Cl distances are significantly different with that to Mo(2) being shorter, the two Mo–C(2A) distances are identical by the 3 σ criterion. The Mo(2)–CNT(2) distance is longer than the Mo(1)–CNT(1) distance. Finally, the Mo(2)–O distance [1.673(3) Å] compares better with those of terminal Mo=O bonds in other cyclopentadienyl complexes of Mo(V), such as 1.684(4) Å for Cp*MoCl₂(O) [35], 1.668(7) Å for [CpMoOCl]₂(μ -O) [36], or 1.676(5) Å for [Cp*MoOCl]₂(μ -O) [37], than with analogous distances in cyclopentadienyl complexes of Mo(IV), such as 1.721(2) Å for (C₅H₄Me)₂Mo(O) [38].

As mentioned above, the structure of this decomposition product is indirect evidence that the borane

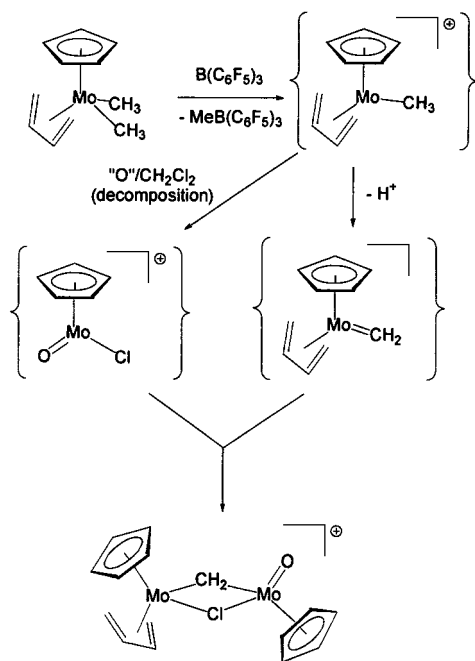
Table 1

Selected bond lengths (Å) and angles (°) for compound [CpMo(η^4 -C₄H₆)(μ -Cl)(μ -CH₂)(O)MoCp][B(C₆F₅)CH₃]^a

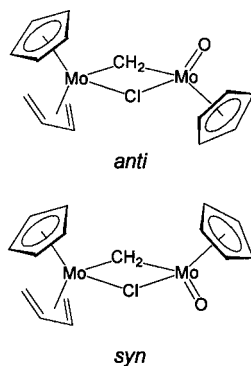
Bond lengths (Å)		Bond angles (°)	
<i>Cation</i>			
Mo(1)–CNT(1)	1.985(4)	CNT(1)–Mo(1)–CNT(3)	130.99(5)
Mo(1)–CNT(3)	1.964(4)	CNT(1)–Mo(1)–Cl	108.22(4)
Mo(1)–Cl	2.497(2)	CNT(1)–Mo(1)–C(2A)	111.80(4)
Mo(1)–C(2A)	2.090(10)	CNT(2)–Mo(2)–Cl	113.25(5)
Mo(1)–C(11)	2.288(5)	CNT(2)–Mo(2)–C(2A)	111.41(4)
Mo(1)–C(12)	2.353(4)	CNT(2)–Mo(2)–O	120.66(7)
Mo(1)–C(13)	2.349(4)	CNT(3)–Mo(1)–C(2A)	99.66(7)
Mo(1)–C(14)	2.298(4)	CNT(3)–Mo(1)–Cl	102.53(5)
C(11)–C(12)	1.409(7)	O–Mo(2)–Cl	102.21(7)
C(12)–C(13)	1.393(7)	O–Mo(2)–C(2A)	105.68(5)
C(13)–C(14)	1.393(6)	Mo(1)–Cl–Mo(2)	72.00(4)
Mo(2)–CNT(2)	2.067(4)	Mo(1)–C(2A)–Mo(2)	86.62(3)
Mo(2)–O	1.673(3)	Mo(1)–Mo(2)–O	107.18(7)
Mo(2)–Cl	2.401(3)	Mo(1)–Mo(2)–CNT(2)	131.99(5)
Mo(2)–C(2A)	2.108(15)	Mo(2)–Mo(1)–CNT(1)	116.74(5)
Mo(1)–Mo(2)	2.8801(5)	Mo(2)–Mo(1)–CNT(3)	112.23(4)
<i>Anion</i>			
B(1)–C(20)	1.659(6)	C(20)–B(1)–C(30)	109.43(3)
B(1)–C(30)	1.662(6)	C(20)–B(1)–C(40)	110.26(3)
B(1)–C(40)	1.656(6)	C(30)–B(1)–C(40)	110.91(3)
B(1)–C(60)	1.658(6)	C(60)–B(1)–C(20)	109.77(3)
		C(60)–B(1)–C(30)	109.01(3)
		C(60)–B(1)–C(40)	107.43(3)

^a CNT(*n*) (*n* = 1, 2) are the center of gravity of the cyclopentadienyl ring [*n* = 1, atoms C(1)–C(5); *n* = 2, atoms C(6)–C(10)]; CNT(3) is the center of gravity of the butadiene ligand [atoms C(11)–C(14)].

reagent has attacked the methyl group rather than the diene ligand in the dimethylmolybdenum(III) precursor, because one methyl group is found to bind the boron atom in the anion, while the putative residual $[\text{CpMo}(\eta^4\text{-C}_4\text{H}_6)(\text{CH}_3)]^+$ becomes incorporated, after deprotonation, into the cationic unit, the methyl ligand becoming the bridging methylene group. The $[\text{Cp-Mo}(\text{O})\text{Cl}]^+$ fragment that completes the structure of the cation must derive from the decomposition of a second molecule of $[\text{CpMo}(\eta^4\text{-C}_4\text{H}_6)(\text{CH}_3)]^+[\text{CH}_3\text{B}(\text{C}_6\text{F}_5)_3]^-$ (see Scheme 1). The high isolated yield (90%) excludes the fact that this complex is a by-product. The formation of the dinuclear cation can be ascribed to the instability of the putative 15-electron intermediate deriving from the methyl abstraction by $\text{B}(\text{C}_6\text{F}_5)_3$. An



Scheme 1.



Scheme 2.

analogous instability has also been observed for related Group 5 complexes, e.g. $[\text{Cp}^*\text{Ta}(\eta^4\text{-C}_4\text{H}_6)\text{Me}]^+$ and $[\text{Tp}'\text{Nb}(\eta^2\text{-PhC}\equiv\text{CMe})\text{Me}]^+$ ($\text{Tp}' =$ hydridotris(pyrazolyl)borate) [7,8,39], which, like our proposed $\text{Mo}(\text{III})$ intermediate, could not be isolated.

Characterization of the title compound is completed by ^1H -, ^{11}B - and ^{19}F -NMR spectroscopy and by mass spectrometry. The ^1H -NMR spectrum (CDCl_3) shows the presence of two different isomers in solution (in a 70:30 ratio by integration of the cyclopentadienyl signals). These two isomers are interpreted as having a different relative position of the $\text{CpMo}(\text{=O})$ and $\text{CpMo}(\eta^4\text{-C}_4\text{H}_6)$ moieties across the central $\text{Mo}_2(\mu\text{-Cl})(\mu\text{-CH}_2)$ moiety, i.e. *syn* or *anti* (see Scheme 2). A similar behavior has been observed for complexes $[\text{CpMo}(\mu\text{-X})(\eta^4\text{-C}_4\text{H}_6)]_2$ ($\text{X} = \text{Cl}, \text{Br}$) [27]. All protons show distinct signals for each isomer, including the six hydrogen atoms of the diene ligand. The two inequivalent methylene protons give rise to two distinct doublets ($J_{\text{HH}} = 10.5$ Hz) for the major isomer, while a singlet is observed for the minor one. The ^{11}B chemical shift and the difference of 2.5 ppm between the *meta*- and *para*-F resonances in the ^{19}F -NMR are in good agreement with the formation of the borate ion and with a significant charge separation in the salt [16,40]. The mass spectrum shows peaks in agreement with the given formulas for the cation and anion in the positive and negative chemical ionization modes, respectively.

3. Conclusion

The borane reagent $\text{B}(\text{C}_6\text{F}_5)_3$ attacks the electron-rich dimethyl complexes $\text{Cp}^*\text{Mo}(\eta^4\text{-diene})\text{Me}_2$ at the methyl position, rather than at the diene ligand, to form relatively stable adducts that resist displacement of the $[\text{CH}_3\text{B}(\text{C}_6\text{F}_5)_3]^-$ anion by Lewis bases. The position of borane attack is suggested by the simulation of the EPR data and indirectly by the structural characterization of the title product. The observed reactivity pattern is consistent with previously available Mulliken charges from DFT computations.

The present study has confirmed the great resistance of the $\text{Mo}(\text{III})\text{-CH}_3$ bond toward heterolytic cleavage, previously shown by the fact that the bond can only be cleaved by acids stronger than H_3O^+ [10]. Yet, compounds of type $\text{Cp}^*\text{Mo}(\eta^4\text{-diene})\text{Me}_2$ has been shown capable of polymerizing ethylene in combination with MAO, with a relatively rapid turnover for the active site. The activation step, however, is difficult [11]. The results shown here will guide us toward the development of modified systems with an improved catalytic activity.

4. Experimental

4.1. General procedures

All reactions were carried out in a Jacomex glove box or by the use of standard Schlenk techniques under an argon atmosphere. The solvents were dried by conventional methods (THF, Et₂O, toluene and pentane from sodium benzophenone ketyl and CH₂Cl₂ from P₄O₁₀) and distilled under argon prior to use. EPR measurements were carried out at the X-band microwave frequency on a Bruker ESP300 spectrometer. The spectrometer frequency was calibrated with DPPH ($g = 2.0037$). NMR spectra were recorded using a Bruker AC-200 or DRX-500. ¹H-NMR spectra were referenced to the residual solvent protons of the deuterated solvent. ¹⁹F- (282.2 MHz) and ¹¹B- (96.2 MHz) NMR spectra were referenced externally to CFCl₃ and BF₃·Et₂O, respectively. Cyclic voltammograms were recorded with an EG&G 362 potentiostat connected to a Macintosh computer through MacLab hardware–software. Electrospray mass spectra were recorded using a Micromass Quattro LC instrument. Isotope patterns were recorded for cation and anion and compared with theoretical patterns using the MASSLYNX 3.5 program. In both cases there was good agreement between the experimental and calculated isotopic mass distributions. The elemental analyses were carried out by the analytical service of the Laboratoire de Synthèse et d'Electrosynthèse Organométallique with a Fisons EA 1108 apparatus. Compound CpMo(diene)Cl₂ were prepared as described in the literature [10]. B(C₆F₅)₃ was prepared as described [41] and was sublimed in vacuo before use.

4.2. Reaction of CpMo(η⁴-C₄H₆)(CH₃)₂ with B(C₆F₅)₃

A solution of CpMo(η⁴-C₄H₆)(CH₃)₂ (84 mg, 0.34 mmol) in toluene (10 ml) was added to a solution of B(C₆F₅)₃ (175 mg, 0.34 mmol) in the same solvent (5 ml) at –20 °C, resulting in an immediate color change from green to orange. The solution was stirred for 15 min at room temperature (r.t.). An aliquot of the solution was examined by EPR, indicating the formation of a new compound (Section 2 and Fig. 1): $g = 1.995$ (multiplet), $a_{\text{Mo}} = 38.91$ G, $a_{\text{H}} = 6.79$ G (3H), $a_{\text{H}} = 4.42$ (3H), $a_{\text{H}} = 4.55$ G (2H), $a_{\text{H}} = 4.55$ G (2H). Cooling the filtered toluene solution to –20 or –80 °C gave either no precipitation or an oil, depending on concentration. The same occurred upon diffusion of pentane into a concentrated (and unfiltered) dichloromethane solution.

4.3. Reaction of CpMo(η⁴-C₄H₄Me₂-2,3)(CH₃)₂ with B(C₆F₅)₃

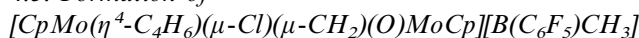
A procedure identical to that described in the previ-

ous section gave rise to the same observations. EPR (toluene): $g = 1.995$ (multiplet), $a_{\text{Mo}} = 34.5$ G. The values of the other hyperfine constants was not optimized by digital fitting. The appearance of this spectrum, however, was essentially identical with that of the butadiene analogue (vide supra), except for a slightly worse resolution.

4.4. Reaction of CpMo(η⁴-C₄H₆)(CH₃)₂ with B(C₆F₅)₃ in the presence of PMe₃

Following the same procedure as described above, PMe₃ (1 ml, 1 M in toluene, 1 mmol) was added via a syringe at r.t. No spectral modification was observed by EPR.

4.5. Formation of



After carrying out a reaction between CpMo(η⁴-C₄H₆)(CH₃)₂ and B(C₆F₅)₃ as indicated above, the toluene solvent was completely evaporated. The residue was then extracted with 3 ml of CH₂Cl₂, followed by filtration through Celite (0.5 × 1 cm). A slow diffusion of pentane in this solution at r.t. afforded red crystals. Yield = 148 mg; 90%. Anal. Calc. for C₃₄H₁₉BClF₁₅Mo₂O: C, 42.16; H, 2.18. Found: C, 41.91; H, 2.09%. Positive Electrospray-MS (Cone: 25 V): $m/z = 441$ ([CpMo(η⁴-C₄H₆)(μ-Cl)(μ-CH₂)(O)MoCp]⁺). Negative Electrospray-MS (Cone: 25 V): $m/z = 526$ ([CH₃B(C₆F₅)₃][–]). ¹H-NMR (CDCl₃, 20 °C, δ): [CH₃B(C₆F₅)₃][–] anion: 0.57 (br.). [CpMo(η⁴-C₄H₆)(μ-Cl)(μ-CH₂)(O)MoCp]⁺ (major isomer): 6.1 (s, 5H, C₅H₅Mo(=O)); 5.6 (s, 5H, C₅H₅Mo(η⁴-C₄H₆)); 8.44 (d, 1H, CH₂, ²J_{H-H} = 10.5 Hz); 7.79 (d, 1H d, CH₂, ²J_{H-H} = 10.5 Hz); 4.80 (m, 1H, C₄H₆); 3.87 (m, 1H, C₄H₆); 3.39 (m, 1H, C₄H₆); 2.74 (m, 1H, C₄H₆); 2.03 (m, 1H, C₄H₆); 1.67 (m, 1H, C₄H₆). [CpMo(η⁴-C₄H₆)(μ-Cl)(μ-CH₂)(O)MoCp]⁺ (minor isomer): 6.05 (s, 5H, C₅H₅Mo(=O)); 5.32 (s, 5H, C₅H₅Mo(η⁴-C₄H₆)); 8.10 (s, 2H, CH₂); 4.54 (m, 1H, C₄H₆); 4.25 (m, 1H, C₄H₆); 3.33 (m, 1H, C₄H₆); 2.83 (m, 1H, C₄H₆); 2.33 (m, 1H, C₄H₆); 1.88 (m, 1H, C₄H₆). ¹¹B-NMR (CDCl₃, 20 °C, δ): –15.3 ppm. ¹⁹F-NMR (CDCl₃, 20 °C, δ): –132.8 (d, *o*-F, ³J_{F-F} = 19.2 Hz), –164.6 (t, *p*-F, ³J_{F-F} = 20.8 Hz), –167.2 (td, *m*-F, ³J_{F-F} = 20.8 Hz, ³J_{F-F} = 19.2 Hz).

4.6. X-ray crystallography for compound



The crystals are air stable and were mounted on the tip of a glass fiber. X-ray diffraction experiments were carried out on a Bruker SMART CCD diffractometer using Mo-K_α radiation ($\lambda = 0.71073$ Å). The data were collected with a frame width of 0.3° in Ω and a counting time of 20 s per frame at a crystal to detector distance

Table 2

Crystal data and structure refinement for [CpMo(η^4 -C₄H₆)(μ -Cl)(μ -CH₂)(O)MoCp)[B(C₆F₅)₃CH₃]

Empirical formula	C ₃₄ H ₁₉ BClF ₁₅ Mo ₂ O
Formula weight	968.63
Temperature (K)	173(2)
Crystal system	Monoclinic
Space group	<i>P</i> 21/ <i>c</i>
Unit cell dimensions	
<i>a</i> (Å)	14.2045(12)
<i>b</i> (Å)	18.5778(14)
<i>c</i> (Å)	13.1036(10)
β (°)	107.380(2)
<i>V</i> (Å ³)	3300.0(5)
<i>Z</i>	4
Absorption coefficient (mm ⁻¹)	0.957
Crystal size (mm ³)	0.113 × 0.044 × 0.016
Theta range for data collection (°)	1.50–30.61
Index ranges	18 ≤ <i>h</i> ≤ 19, –26 ≤ <i>k</i> ≤ 16, –18 ≤ <i>l</i> ≤ 18
Reflections collected	26 693
Independent reflections	9775 [<i>R</i> _{int} = 0.0792]
Observed independent reflections [<i>I</i> > 2σ(<i>I</i>)]	4995
Completeness to $\theta = 30.61^\circ$	96.1%
Goodness-of-fit on <i>F</i> ²	0.914
Final <i>R</i> indices [<i>I</i> > 2σ(<i>I</i>)]	<i>R</i> ₁ = 0.0485 ^a , <i>wR</i> ₂ = 0.0870 ^b
<i>R</i> indices (all data)	<i>R</i> ₁ = 0.1340, <i>wR</i> ₂ = 0.1066
Largest difference peak and hole (e. Å ⁻³)	0.718 and –0.552

$$^a R_1 = \frac{\sum ||F_o| - |F_c||}{\sum F_o}$$

$$^b wR_2 = \frac{[\sum [w(F_o^2 - F_c^2)] / \sum [w(F_o^2)]]^{1/2}}$$

of 4 cm. The software SAINT [42] was used for integration of intensity reflections and scaling and SADABS [43] for absorption correction. Final cell parameters were obtained by global refinement of reflections obtained from integration of all the frame data. The crystal parameters and basic information relating data collection and structure refinement for compound [CpMo(η^4 -C₄H₆)(μ -Cl)(μ -CH₂)(O)MoCp)[B(C₆F₅)₃CH₃] are summarized in Table 2. The structure was solved by direct methods and refined by the full-matrix method based on *F*² using the SHELXTL software package [44]. The nonhydrogen atoms were refined anisotropically; the positions of all hydrogen atoms were generated geometrically, assigned isotropic thermal parameters and allowed to ride on their respective parent carbon atoms. The chlorine and methylene bridge are disordered and were refined with a occupations factors of 0.62 for C11 and C2A and 0.38 for C12 and C1A.

5. Supplementary material

Crystallographic data for the structural analysis have been deposited with the Cambridge Crystallographic Data Centre, CCDC No. 164163 for compound [CpMo(η^4 -C₄H₆)(μ -Cl)(μ -CH₂)(O)MoCp)[B(C₆F₅)₃-

CH₃]. Copies of this information may be obtained free of charge from The Director, CCDC, 12 Union Road, Cambridge, CB2 1EZ UK (Fax: +44-1223-336033; e-mail: deposit@ccdc.cam.ac.uk or www:http://www.ccdc.cam.ac.uk).

Acknowledgements

We are grateful to the CNRS (Programme Catalyse pour l'Industrie et l'Environnement) and COST D17 (Working group on 'Environmentally friendly catalysts for olefin polymerization') for support of this work. E.L.G. thanks the MENRT for a doctoral fellowship. Thanks are also extended to the Servei Central d'Instrumentació Científica (CSIC) of the university Jaume I for providing us with mass spectrometry and X-ray facilities.

References

- [1] R.F. Jordan, *Adv. Organomet. Chem.* 32 (1991) 325.
- [2] P.C. Mohring, N.J. Coville, *J. Organomet. Chem.* 479 (1994) 1.
- [3] H.H. Brintzinger, D. Fischer, R. Mülhaupt, B. Rieger, R.M. Waymouth, *Angew. Chem. Int. Ed. Engl.* 34 (1995) 1143.
- [4] M. Bochmann, *J. Chem. Soc. Dalton Trans.* (1996) 255.
- [5] W. Kaminsky, *J. Chem. Soc. Dalton Trans.* (1998) 1413.
- [6] K. Mashima, S. Fujikawa, H. Urata, E. Tanaka, A. Nakamura, *J. Chem. Soc. Chem. Commun.* (1994) 1623.
- [7] K. Mashima, S. Fujikawa, Y. Tanaka, H. Urata, T. Oshiki, E. Tanaka, A. Nakamura, *Organometallics* 14 (1995) 2633.
- [8] J. Jaffart, C. Nayral, R. Choukroun, R. Mathieu, M. Etienne, *Eur. J. Inorg. Chem.* (1998) 425.
- [9] E. Le Grogneq, R. Poli, L.-S. Wang, *Inorg. Chem. Commun.* 2 (1999) 95.
- [10] E. Le Grogneq, R. Poli, P. Richard, *Organometallics* 19 (2000) 3842.
- [11] E. Le Grogneq, R. Poli, *Chem. Eur. J.* in press.
- [12] E.Y.-X. Chen, T.J. Marks, *Chem. Rev.* 100 (2000) 1391.
- [13] X. Yang, C.L. Stern, T.J. Marks, *J. Am. Chem. Soc.* 116 (1994) 10015.
- [14] M. Bochmann, S.J. Lancaster, M.B. Hursthouse, K.M.A. Malik, *Organometallics* 13 (1994) 2235.
- [15] G.C. Bazan, W.D. Cotter, Z.J.A. Komon, R.A. Lee, R.J. Lachicotte, *J. Am. Chem. Soc.* 122 (2000) 1371.
- [16] A.D. Horton, J. de With, A.J. van der Linden, H. van der Weg, *Organometallics* 15 (1996) 2672.
- [17] F. Amor, A. Butt, K.E. du Plooy, T.P. Spaniol, J. Okuda, *Organometallics* 17 (1998) 5836.
- [18] J.S. Rogers, X. Bu, G.C. Bazan, *J. Am. Chem. Soc.* (2000) 730.
- [19] B. Temme, G. Erker, J. Karl, H. Luftmann, R. Fröhlich, S. Kotila, *Angew. Chem. Int. Ed. Engl.* 34 (1995) 1755.
- [20] B. Temme, J. Karl, G. Erker, *Chem. Eur. J.* 2 (1996) 919.
- [21] J. Karl, M. Dahlmann, G. Erker, K. Bergander, *J. Am. Chem. Soc.* 120 (1998) 5643.
- [22] G. Jimenez Pindado, S.J. Lancaster, M. Thornton-Pett, M. Bochmann, *J. Am. Chem. Soc.* 120 (1998) 6816.
- [23] A.D. Cowley, G.S. Hair, B.G. McBurnett, R.A. Jones, *Chem. Commun.* (1999) 437.
- [24] M. Dahlmann, G. Erker, R. Fröhlich, O. Meyer, *Organometallics* 19 (2000) 2956.

- [25] J.L. Davidson, K. Davidson, W.E. Lindsell, *J. Chem. Soc. Chem. Commun.* (1983) 452.
- [26] J.L. Davidson, K. Davidson, W.E. Lindsell, N.W. Murrall, A.J. Welch, *J. Chem. Soc. Dalton Trans.* (1986) 1677.
- [27] L.-S. Wang, J.C. Fettingler, R. Poli, *J. Am. Chem. Soc.* 119 (1997) 4453.
- [28] R. Poli, L.-S. Wang, *Polyhedron* 17 (1998) 3689.
- [29] E. Le Grogneć, J. Claverie, R. Poli, *J. Am. Chem. Soc.* in press.
- [30] X. Yang, C.L. Stern, T.J. Marks, *J. Am. Chem. Soc.* 113 (1991) 3623.
- [31] C.L. Beswick, T.J. Marks, *Organometallics* 18 (1999) 2410.
- [32] A.J. Sillanpää, K.E. Laasonen, *J. Am. Chem. Soc.* 20 (2001) 1334.
- [33] H.C. Strauch, G. Erker, R. Fröhlich, *Organometallics* 17 (1998) 5746.
- [34] H.C. Strauch, G. Erker, R. Fröhlich, M. Nissinen, *Eur. J. Inorg. Chem.* (1999) 1453.
- [35] J.M.B. Blanchard, Q. Chen, Y.-D. Chang, M.B. Sponsler, *Inorg. Chim. Acta* 221 (1994) 147.
- [36] F. Bottomley, E.C. Ferris, P.S. White, *Organometallics* 9 (1990) 1166.
- [37] K. Umakoshi, K. Isobe, *J. Organomet. Chem.* 395 (1990) 47.
- [38] N.D. Silavwe, M.Y. Chiang, D.R. Tyler, *Inorg. Chem.* 24 (1985) 4219.
- [39] K. Mashima, S. Fujikawa, A. Nakamura, *J. Am. Chem. Soc.* 115 (1993) 10990.
- [40] A.D. Horton, J. de With, *Organometallics* 16 (1997) 5424.
- [41] A.G. Massey, A.J. Park, *J. Organomet. Chem.* 2 (1964) 245.
- [42] Bruker Analytical X-ray System, SAINT, version 5.0, Madison, WI, 1998.
- [43] G.M. Sheldrick, SADABS empirical absorption program, University of Göttingen, 1996.
- [44] G.M. Sheldrick, SHELXTL, version 5.1, Bruker AXS, Inc., Madison, WI, 1997.